HHS Public Access

Author manuscript

J Pathol. Author manuscript; available in PMC 2024 July 01.

Published in final edited form as:

J Pathol. 2023 July ; 260(3): 339–352. doi:10.1002/path.6086.

Kisspeptin regulates airway hyperresponsiveness and remodeling in a mouse model of asthma

Niyati A. Borkar[†],

Nilesh Sudhakar Ambhore[†],

Premanand Balraj[†],

Yogaraj S. Ramakrishnan[†],

Venkatachalem Sathish[*]

Department of Pharmaceutical Sciences, School of Pharmacy, College of Health Professions, North Dakota State University, Fargo, ND, USA.

Abstract

Asthma is a multifactorial disease of origin characterized by airway hyperresponsiveness (AHR) and airway remodeling. Several pieces of evidence from other pathologies suggest that Kisspeptins (Kp) regulate cell proliferation, migration, and invasion, mechanisms that are highly relevant to asthma. Our recent *in vitro* studies show Kp-10 (active peptide of Kp), via its receptor, KISS1R, inhibits human airway smooth muscle cell proliferation. Here, we hypothesize a crucial role for Kp-10 in regulating AHR and airway remodeling *in vivo*. Utilizing C57BL/6J mice, we assessed the effect of chronic intranasal Kp-10 exposure on mixed allergen (MA)-induced mouse model of asthma. MA-challenged mice showed significant deterioration of lung function compared to those exposed to vehicle (DPBS); Kp-10 treatment significantly improved the MA-altered lung functions. Mice treated with Kp-10 alone did not show any notable changes in lung functions. MA-exposed mice showed significant reduction in KISS1R expression as compared to vehicle alone. MA-challenged mice showed significant alterations in immune cell infiltration in the airways and remodeling changes. Pro-inflammatory cytokines were significantly increased upon MA exposure, an effect abrogated by Kp-10 treatment. Furthermore, biochemical and histological studies showed Kp-10 exposure significantly reduced MA-induced smooth muscle mass and soluble collagen in the lung. Overall, our findings highlight the effect of chronic Kp-10 exposure in regulating MA-induced AHR and remodeling.

Keywords

Airway smooth muscle; Kisspeptin receptor; Airway inflammation; Lung mechanics; flexiVent; Mixed allergens; Sex-steroids; Vimentin; α-smooth muscle actin

[*]**Correspondence to:** V Sathish, Department of Pharmaceutical Sciences, North Dakota State University, Fargo, ND 58102, USA. s.venkatachalem@ndsu.edu.

[†]Equal contributions

Author contributions statement

VS, NSA, NAB, and PB contributed to study concept and design. NAB, NSA, PB, and YSR acquired data. NAB, NSA, YSR, and PB analyzed and interpreted the data. NAB, NSA, PB, YSR, and VS drafted and edited the manuscript. All authors approved the final version of the manuscript.

No conflicts of interests were declared.

Introduction

Asthma is a common chronic airway disorder resulting as a consequence of airway inflammation, hyperreactivity and remodeling, affecting almost 300 million people worldwide [1–4]. Factors such as sex, age, disease status and smoking play a critical role in exacerbating asthma [5–7]. Asthma may affect people of any age, although it is more common in females than males, as outlined by multiple studies [8–11]. A crucial finding in all studies suggests the post-pubertal reversal of asthma occurrence; with women showing increased susceptibility to asthma as compared to men [12,13]. Several research groups have addressed these concerns in multiple clinical and epidemiological studies, although the underlying factors behind these differences are still unexplained. Therefore, it is understandable that mechanisms regulating these sex differences in asthma originate upstream of or independent of sex steroids, especially estrogen. Hence, it is important to identify other alternative pathways upstream of sex steroids in the context of the sex-specific occurrence of asthma. With this understanding, a candidate of interest for our investigations is the family of Kisspeptins (Kp). Kp are encoded by the *KISS1* gene located on chromosome 1q32.1 and upon proteolytic cleavage, Kp produces multiple cleaved peptides including 54-, 14-, 13-, and 10-amino acid peptides, which all share the common amidated C-terminus 10 amino-acid sequence [14]. The G-protein coupled receptor 54 or KISS1R serves as the receptor for Kp [14,15]. Multiple studies have elucidated the role of Kp/KISS1R in different organs such as the pancreas, breast, bladder, brain, ovaries, and liver [14,16,17]. Evidence from the CNS and other organs as mentioned earlier justify our rationale to investigate Kp as a potential upstream modulator of sex steroids that could be relevant to the airways as: A) Kp is a critical initiator of puberty and ovulation via central control of the hypothalamic-pituitary-gonadotropic axis [18,19]; B) Kp regulates release and secretion of gonadotropin-releasing-hormone and gonadal sex steroids [20–22]; and C) the KISS1R agonist, metastin has been used a treatment option for sex steroid dependent diseases [23]. Our group recently reported the expression of Kp and KISS1R in the human lung, specifically in the airway smooth muscle (ASM) suggesting a potential role of Kp/KISS1R signaling in the airways. We observed lesser expression of Kp and KISS1R in ASM cells from asthmatic as compared to non-asthmatic individuals [24]. We showed further that the KISS1R agonist Kp-10 ablates platelet-derived growth factor (PDGF)-induced proliferation in ASM cells via inhibition of ERK and P38/MAPK signaling pathways [24]. However, the role of Kp in an *in vivo* model of asthma has not been investigated until now. To integrate our *in vitro* findings and to understand the role of Kp/KISS1R in lung physiology in the context of asthma, we have employed a mixed allergen (MA)-induced mouse model of asthma.

Our results reveal for the first time the importance of Kp/KISS1R signaling *in vivo,* thus corroborating our *in vitro* findings. The primary objective of this study was to determine the effect of Kp-10 in regulating lung function parameters during airway hyperresponsiveness (AHR) and remodeling in a chronic MA-induced mouse model of asthma. As a secondary objective, we included ovariectomized (OVX) mice in the study population to dissect the effects of endogenous estrogen in the presence of exogenously administered Kp-10. Thus,

the knowledge gained from this study provides relevance for Kp/KISS1R signaling in the airway structure affecting function in the context of asthma.

Materials and methods

Experimental animals

All animal study protocols were approved by the Institutional Animal Care and Use Committee (IACUC) at North Dakota State University and experiments were conducted as approved under the guidelines of "National Institutes of Health Guide for the Care and Use of Laboratory Animals" [25]. Wild-type (WT) breeding pairs of C57BL/6J background female and male mice were procured from The Jackson Laboratory, Bar Harbor, ME, USA. We carried out in-house breeding and the resultant mice were used at 6–8-weeks of age. Age-matched C57BL/6J background OVX mice were obtained from The Jackson Laboratory. All animals were housed under appropriate temperatures with 12 h light and 12 h dark cycles. The animals were provided with food and water *ad libitum*. Mice from male, female and OVX populations were allocated with a minimum of 6 mice per treatment group: 1) Vehicle (Dulbecco's Phosphate Buffered Saline, DPBS-challenged); 2) Mixed allergen (MA)-Challenged; 3) Kp-10 (Metastin 45–54, sc-221884 obtained from Santa Cruz Biotechnology, Inc. Dallas, TX, USA); 4) Kp-10+MA.

Mixed allergens and reagents

Ovalbumin from chicken egg white was from Sigma-Aldrich (St. Louis, MO, USA). The allergens comprising *Alternaria alternata, Aspergillus fumigatus,* and *Dermatophagoides farinae* (House dust mite) were purchased from Greer laboratories, Lenoir, NC, USA. DPBS (Cat# 14190–144) and protease and phosphatase inhibitor (PPI) cocktail (Cat# 1861284) were purchased from Thermo Fisher Scientific, Waltham, MA, USA.

Mixed allergen challenge and treatments

Mice from all three populations (male, female, and OVX) were assigned to MA groups and a mixture of four allergens containing 10 μg each of ovalbumin, *Alternaria alternata*, *Aspergillus fumigatus* and *Dermatophagoides farina* in 25 μl of DPBS were administered intranasally on alternate days (starting from day 1) for 4 weeks (3 days/week) as previously described [26–28]. Animals in the vehicle group received an equal volume (25 μl) of DPBS alone for the same time durations. From day 2, mice from all three study populations received Kp-10 (1.17 mg/kg) [29] in 25 μl of DPBS intranasally on alternate days (3 days/week). Administration of Kp-10 and MA were performed under isoflurane anesthesia. Please refer to the schematic in Figure 1A for additional details.

Lung function analysis

Mice were assessed using a flexiVent system (Scireq, Montreal, Canada) on day 29, and parameters such as total respiratory system resistance (Rrs), compliance (Crs), and elastance (Ers) were recorded as per the previously described method [26–28]. Ketamine (100 mg/kg i.p.) and xylazine (10 mg/kg i.p.) were used for anesthesia. Rrs, Crs, and Ers were recorded at baseline (0 mg/ml Methacholine, MCh) and increasing doses of nebulized MCh (6.25–

50.0 mg/ml). Max Rrs and Crs values at 50 mg/ml of MCh was used to compare the effectiveness between treatment groups.

Bronchoalveolar lavage fluid (BALF) processing and tissue collection

Following lung function analysis, BALF was obtained by injecting 1.0 ml of DPBS (supplemented with PPI cocktail) via the tracheal cannula, with about 600 μl of fluid recovered. The collected BALF was stored at −80 °C until analysis. Following this, we perfused the lungs with 10 ml of DPBS via the right ventricle to eliminate circulating blood before collecting each lobe. The left lobe of each mouse lung was stored in Carnoy's solution (100% Ethanol, Chloroform, and Glacial acetic acid in a ratio of 6:3:1 with ferric chloride, Sigma-Aldrich) for a few hours, followed by replacement of the solution with 70% ethanol and preparation for histology studies [30,31].

Cytokine ELISA multiplex assay in BALF

BALF was centrifuged briefly and then aliquoted into 0.5–0.6 ml microcentrifuge tubes for further analysis [31]. Samples were subsequently processed following the manufacturer's protocol (Eve Technologies Pvt. Ltd, Calgary, Canada).

Histopathology analyses

The stored left lung lobes were embedded in paraffin wax blocks and sections were stained using H&E (Sigma-Aldrich), PAS (EMS, Hatfield, PA, USA) and Masson's trichrome (Chondrex, Redmond, WA, USA), using previously described techniques [26,27]. The slides were then scanned using Epredia Pannoramic MIDI II 20x (3DHISTECH, Budapest, Hungary). The scanned H&E sections were examined for inflammatory cell recruitment by determining the optical density (O.D.) around the airways using ImageJ (National Institutes Health, USA, https://imagej.net/software/fiji/; downloaded 04 November 2022). The PAS-stained sections were analyzed for mucin expression by counting the number of PAS-positive epithelial cells in the airways with approximately similar diameters (~50 μm). Results are expressed as the percentage cells per airway that were PAS-positive [32]. Collagen was stained with Masson's trichrome and the positively-stained area around the airways was measured using ImageJ. The collagen area was then normalized for airway size (collagen area μm^2/airway perimeter μm) as previously described [33].

Western blotting of lung tissue homogenates

Fresh lung tissue samples (10 mg) were collected and homogenized in sucrose buffer (100 μl) in the presence of a PPI cocktail. Total protein was estimated and at least 40 μg of protein was loaded in each well/sample for SDS-PAGE. Western blot analyses were carried out following published protocols [34]. The blots were probed for Kp (Cat# sc-101246, 1:200; Santa Cruz Biotechnology), KISS1R (Cat# PA5–49719, 1;1000; Invitrogen, Waltham, MA USA), Vimentin (Cat# V5255, 1;1000; Sigma-Aldrich), α-smooth muscle actin (α-SMA, Cat# A2547, 1:1000; Sigma-Aldrich.), and β-actin (Cat# G043, 1:2000; Applied Biological Materials, Richmond, Canada) followed by scanning in LI-COR near infra-red imaging system (LI-COR Biosciences, Lincoln, NE, USA). The LI-COR NIR labeled secondary antibodies were used to determine the intensity and densitometric analysis was performed

using Image studio software v5.2.5 (LI-COR Biosciences). Ratios for each sample were obtained by dividing raw values for proteins of interest with the values for β-actin. Group ratios were then normalized to those for the vehicle and presented as a relative protein expression.

Laser-Capture Microdissection (LCM) assisted ASM isolation and RT-PCR

LCM was performed following the technique established previously in our laboratory [27,35] using a Zeiss-Axio Imager Z1 PALM Microbeam laser capture microscope system (Zeiss, Thornwood, NY, USA). ASM were identified and marked using Palm-Robo software and a laser cut was performed to catapult the specific ASM cells into an RNAase-free microtube containing single cell PicoPure RNA extraction buffer. RNA was isolated from the collected cells using the PicoPure® RNA Isolation Kit (Thermo Fisher Scientific) and stored at −80 °C for further studies [35]. Representative images for isolation of ASM from the mouse airways using LCM are shown in supplementary material, Figure S1. RT-PCR was performed using BrightGreen 2X qPCR Master Mix (Applied Biological Materials, MasterMix-S-XL) and QuantStudio 3 RT-PCR system (Thermo Fisher Scientific) following the manufacturer's instructions. The fold-changes in mRNA expressions were calculated by normalization of the Ct values of target genes to reference gene s16 using the ΔΔCt method [34,35]. Supplementary material, Table S1 lists the primer sequences used for RT-PCR analysis.

Soluble collagen assay

Whole lung tissue lysates were used to measure the level of soluble collagen as an important marker for lung tissue remodeling. This assay was performed following the manufacturer's protocol (Sircol Soluble Collagen Assay, Biocolor Life Science Assay, Carrickfergus, UK) and a previously described technique [36,37]. Final absorbance values were measured at 556 nm using a Synergy HTX Plate Reader (Biotek, Winooski, VT, USA).

Statistical analysis

All the experimental groups consisted of a minimum of six mice. Statistical analysis was performed using an unpaired *t*-test or one-way repeated measures ANOVA or two-way ANOVA followed by Tukey's *post hoc* test for multiple comparisons using GraphPad Prism version 9.1.0 (GraphPad Software, San Diego, CA, USA). Data are expressed as mean ± SEM with statistical significance tested at a minimum of $p<0.05$ level.

Results

Kp/KISS1R protein and mRNA expression in the lung

The experimental design of the study is presented in Figure 1A. The protein expression of Kp and KISS1R in the lung tissue homogenate was measured by western blot analysis. There was no significant difference observed for the expression of Kp in the lung homogenates of MA-challenged male, female and OVX mice (Figure 1B–D) compared to the respective DPBS-challenged mice. Interestingly, the expression of KISS1R was significantly downregulated in the lung homogenates of mice from MA-challenged groups in all three study populations ($p<0.01$ for male and OVX, $p<0.001$ for female, Figure 1E–G)

compared to the respective DPBS-challenged mice. LCM was used to isolate ASM layers and treatment group RNA was isolated. RT-PCR analysis showed a significant reduction in ASM-specific *Kiss1* mRNA ($p<0.05$ for male and female; $p<0.01$ for OVX, Figure 1H–J) and *Kiss1r* mRNA ($p<0.01$ for male and OVX; $p<0.001$ for female, Figure 1K–M) expression in MA-challenged mice from all the study populations compared to the respective DPBS challenged mice.

Effect of Kp-10 on total respiratory system resistance (Rrs)

We assessed the effects of chronic exogenous Kp-10 *in vivo* using the forced oscillation technique of the flexiVent FX1 module to measure Rrs, which represents airway constriction. Male, female, and OVX mice showed an increase in Rrs in response to inhaled increased methacholine concentrations (MCh; 0–50 mg/ml) in the MA-challenged group compared to DPBS-challenged mice (Figure 2A–C). To compare the effectiveness of treatments, we used Max Rrs at the concentration of 50 mg/ml of MCh (Figure 2D–F). MA-challenged male, female and OVX mice showed a significant increase in Max Rrs ($p<0.001$). Mice treated with Kp-10 alone did not show any significant changes in Max Rrs in all three study populations compared with mice from the respective DPBS group. However, MA-challenged mice, treated with Kp-10 showed a significant reduction in Max Rrs in male ($p<0.001$), female ($p<0.001$), and OVX ($p<0.05$) mice compared to respective MA-challenged mice (Figure 2D–F). In the comparison of all three study populations, male ($p<0.001$) and female ($p<0.001$) mice tended to show a profound effect of Kp-10 on the reduction in MA-induced Rrs, while OVX ($p<0.05$) mice showed minimal effects.

Effect of Kp-10 on total respiratory system compliance (Crs)

Crs was measured for the lungs of mice exposed to MA and the effect of Kp-10 was assessed in the respective treatment groups. Mice exposed to MA showed a decrease in Crs in all the study populations compared with DPBS-challenged mice (Figure 3A–C). Max Crs in response to 50 mg/ml MCh was used to compare the effectiveness of Kp-10 in the different study populations (Figure 3D–F). MA-challenged mice showed a significant reduction in Max Crs as compared to mice receiving DPBS alone across all the study populations ($p<0.001$). Mice treated with Kp-10 alone did not show any significant changes in Max Crs compared to the respective DPBS group. MA-challenged mice, treated with Kp-10 showed a significant increase in Max Crs in male ($p<0.05$), female ($p<0.05$) and OVX ($p<0.01$) mice compared to respective MA-challenged mice (Figure 3D–F).

Effect of Kp-10 on total respiratory system elastance (Ers)

Ers was measured for the lungs of MA-challenged mice and the effect of Kp-10 was assessed in the respective treatment groups. We observed an increase in Ers in male, female, and OVX MA-challenged mice compared with DPBS (supplementary material, Figure S2A–C). Max Ers in response to 50 mg/ml MCh was used to compare the effectiveness of the treatments (supplementary material, Figure S2D–F). MA-challenged mice showed a significant increase in Max Ers as compared to mice exposed to DPBS alone across all the study populations ($p<0.001$). Mice treated with Kp-10 alone, for all three study populations, did not show any significant changes compared to the DPBS group. MA-challenged mice treated with Kp-10 showed a significant reduction in Max Ers for males and females

(p<0.001, supplementary material, Figure S2D,E) compared to MA-challenged mice. MA-challenged OVX mice treated with Kp-10 tended to show a decrease in Max Ers, albeit not significant (supplementary material, Figure S2F).

Effect of Kp-10 on the cytokine milieu of BALF

Activation of Th2 cells due to allergen exposure leads to the production of inflammatory cytokines, which subsequently contribute to AHR. To determine Kp-10's effect on the inflammatory milieu, we measured cytokines levels in the BALF lungs of male, female and OVX mice. MA-challenged mice showed a significant increase in the cytokine levels in all three study populations, as evidenced by increased levels of IL-1α (p<0.001 for male and female, p<0.01 for OVX; Figure 4A), IL-1β (p<0.001, for all three study populations; Figure 4B), IL-2 (p<0.001 for male and female, p<0.05 for OVX; Figure 4C), IL-4 (p<0.001 for all three study populations; Figure 4D), IL-5 (p<0.001 for all three study populations; Figure 4E), IL-6 (p<0.001 for all three study populations; Figure 4F), keratinocyte-derived chemokine (KC, p<0.001 for all three study populations; Figure 4G), and TNF-α (p<0.001 for all three study populations; Figure 4H). Furthermore, mice treated with Kp-10 showed significant suppression of MA-induced increases in cytokine levels for IL-1α (p<0.05 for male and OVX, p<0.01 for female; Figure 4A), IL-1β (p<0.05 for male, p<0.001 for female, p<0.01 for OVX; Figure 4B), IL-2 (p<0.01 for male, p<0.001 for female, p<0.05 for OVX; Figure 4C), IL-4 (p<0.01 for male and female, p<0.001 for OVX; Figure 4D), IL-5 (p<0.001 for male and female, p<0.01 for OVX; Figure 4E), IL-6 (p<0.01 for male, p<0.001 for female and OVX; Figure 4F), KC (p<0.001 for female; Figure 4G), and TNF-α (p<0.01 for male, p<0.001 for female and OVX; Figure 4H). Notably, Kp-10 treatment alone (compared with DPBS treated groups) did not show any significant changes for all of the cytokines measured in the BALF. Overall, these data demonstrate that a MA challenge significantly altered BALF cytokine levels in all three study populations. Here, Kp-10 treatment significantly ablated MA-induced increases in cytokine levels in all three study populations, with female mice tending to show a better effect of Kp-10 in reducing MA-induced upregulation in cytokine levels.

Effect of Kp-10 on airway structure and morphology

To integrate the observed changes in the lung mechanics and cytokine milieu with airway structural changes, we performed histological analysis using H&E (Figure 5A), PAS (Figure 5C), and Masson's Trichrome stains (Figure 5E). H&E-stained sections showed a significant increase in inflammatory cells recruitment in the airways of MA-challenged mice (p<0.001 for all male, female and OVX mice) compared with respective DPBS-challenged mice (Fig.5B). Furthermore, MA-challenged mice treated with Kp-10, showed a significant reduction in the recruitment of inflammatory cells (p<0.001 for male, female and OVX mice) compared to MA-challenged group. The mucin production in airway epithelial cells was also detected using PAS staining across the study population for respective treatment groups. The production of mucin was significantly increased in the airway epithelial cells of MA-challenged mice (p<0.001 for male, female, and OVX mice) compared with respective DPBS-challenged mice (Figure 5D). Notably, MA-induced mucin production in airway epithelial cells was reduced upon Kp-10 treatment in mice from all three study populations (p<0.001 for male, female and OVX). Furthermore, Masson's Trichrome stained

sections showed increased collagen deposition around the airways in MA-challenged mice ($p<0.001$ for male, female and OVX) compared with the respective DPBS-challenged mice (Figure 5F). Here, MA-challenged mice treated with Kp-10 showed reductions in collagen deposition around the airways in the lung sections of all study populations ($p<0.001$ for male, $p<0.05$ for female, and $p<0.01$ for OVX).

Effect of Kp-10 on α-smooth muscle actin (α-SMA) and vimentin in the lung

α-SMA often considered as a characteristic marker for smooth muscle and was found to be increased during airway remodeling [38]. Vimentin is an intermediate filament protein involved in phenotype changes during lung fibrosis [26,28]. Western analyses of lung homogenates from MA-challenged mice showed a significant increase in the expression of α-SMA ($p<0.05$ for male, female and OVX; Fig.6A–C) and vimentin ($p<0.01$ for male; $p<0.05$ for female and OVX; Figure 6D–F) expression in all three study populations compared to the respective DPBS-challenged mice. There were no significant changes in α-SMA and vimentin protein expression with exposure to Kp-10 alone when compared to DPBS-challenged groups. Interestingly, MA-challenged mice treated with Kp-10 showed significant downregulation of α-SMA ($p<0.05$ for male and OVX; $p<0.01$ for female; Figure 6A–C) and vimentin ($p<0.01$ for male; $p<0.05$ for female and $p<0.001$ for OVX; Figure 6D–F). In addition, the accumulation of collagen in the whole lung tissue samples of different treatment groups were determined using the sircol soluble collagen assay. In MA-challenged mice, we observed a significant increase in the soluble collagen content of the lungs of male ($p<0.01$; Figure 6G), female ($p<0.001$; Figure 6H) and, OVX ($p<0.001$; Figure 6I) mice compared with the respective DPBS-challenged mice. Treatment with Kp-10 alone showed no significant changes in soluble collagen content compared with the respective DPBS-challenged groups. MA-challenged mice treated with Kp-10 had significantly reduced soluble collagen content ($p<0.01$ for male, female and OVX; Figure 6G–I) compared to the respective MA-challenged groups.

Discussion

Asthma is a heterogeneous disorder of airways mainly associated with chronic airway inflammation, reduced lung functions, tissue remodeling, and AHR [3,8,9,11,26,27]. Several studies have investigated the causative factors as well as the underlying mechanisms responsible for airway inflammation, revealing a broad spectrum of variables [2,7,39]. In contrast, few studies have focused on airway remodeling associated with ASM, which results in chronic airway obstructive changes. Here, the ASM is very crucial considering its role in controlling the secretion of inflammatory cytokines, extracellular matrix (ECM)/remodeling and other growth mediators [7,40,41].

Kisspeptins (Kp) belong to a family of neuropeptides and originate from a common precursor, prepro-kisspeptin to produce smaller amidated cleaved peptides of different amino acid chain lengths- Kp-10, Kp-13, Kp-14 and Kp-54 [14,16,17,42]. Kp regulate gonadotropin secretion in several mammalian species, acting via KISS1R. Numerous studies have delineated the anti-metastatic and tumor-suppressant role of Kp/KISS1R signaling, which are found to inhibit NF-kB and MAPK signaling pathways [43–48]. We demonstrated

the *in vitro* role of Kp via activation of its receptor, KISS1R, in regulating ASM proliferation and observed that cleaved forms of Kp, mainly Kp-10, alleviated PDGF-induced ASM proliferation by regulating the p38/MAPK signaling pathways [24]. Thus, laying the foundation for our current *in vivo* study exploring the role of Kp in a MA-induced mouse model of asthma. Previous studies established the pharmacokinetic profiling of Kp using *in vivo* mouse models [49]. Additionally, *in vitro* studies show receptor binding affinities and cell signaling properties for all cleaved fragments of Kp [50]. Based on previous *in vivo* mouse study [29] and from our *in vitro* findings, we selected a single dose of Kp-10 in the current study.

We used the MA-induced mouse model of asthma, which is a robust and effective asthma model that features Th2-biased eosinophilic inflammation, airway remodeling, and similar pathological manifestations that resemble those observed in human asthma [30]. Previous studies have reported that 17β-estradiol (E_2) regulates Kp/KISS1R signaling through E_2-dependent transcriptional activation of the *K1SS1* gene in female mice [51,52]. To isolate the effect of Kp/KISS1R signaling from endogenous E_2, we used OVX mice in our study.

We observed reduced KISS1R expression in lung tissue homogenates from all MA-challenged mice, implying the altered or impaired protective Kp/KISS1R signaling in the lungs during asthmatic conditions. This aligns with our previous *in vitro* studies, where we observed decreased expression of KISS1R in asthmatic ASM cells [15,24]. Our lung mechanics studies using the flexiVent system indicated a higher Rrs and Ers, with reduced Crs in MA-challenged mice from all three study populations as shown previously [26–28]. The increase in Rrs and Ers were of a similar magnitude in MA-challenged mice, which is indicative of AHR. This is consistent with previous observations where Rrs and Ers were found to be higher in sensitized mice as compared to unsensitized mice [26–28]. While Rrs reflects the overall airway obstruction and stiffness, Ers is a measure of the elastic stiffness of the respiratory system that is changed by recruitment or decruitment of airways [53,54]. The lower Crs most likely relates to luminal narrowing due to increased airway wall thickening with changes in the cellular components [55]. This is consistent with our observation showing increased α-SMA and vimentin in the MA-challenged mice, that were attenuated with Kp-10 treatment. Interestingly, with a reduced lung KISS1R expression observed in asthmatic conditions, exogenous Kp-10 exposure mitigated MA-induced AHR, emphasizing the crucial role of Kp/KISS1R signaling in lung pathophysiology.

Multiple lines of evidence support that during severe lung inflammation, activation of numerous inflammatory/structural cells occurs, and each secretes cytokines or chemokines to modulate lung structure and function [7,56,57]. These effects are most likely regulated by the release of inflammatory cytokines from different effector T cells such as Th1/Th2 and Th17. In our study, we measured inflammatory cytokines levels in BALF fluid from the MA-challenged mice with or without Kp-10 treatment. As expected, we observed upregulated levels of the inflammatory cytokines IL-1α, IL-1β, IL-2, IL-4, IL-5, IL-6, TNF-α and KC in asthmatic mice. Here, female mice elicited higher Th2 cytokines levels, whereas there was no significant change in Th1 cytokine levels compared to MA-challenged male and OVX mice. This observed difference could be due to the differential regulation of Th1/Th2 cytokines production by estrogens, which is consistent with previous studies

[26,28]. Interestingly, the decreased expression of Th2 cytokine levels from allergic male mice signifies the predominant role of androgens in the suppression of Th2 dominant inflammatory responses [26]. The cytokine levels of MA-challenged OVX mice tended to be lower compared to other groups, the absence of female sex hormones in OVX mice may have led to an impairment of effector T cell activation. Moreover, we noticed that in all MA-challenged groups, levels of IL-1α and IL-1β were upregulated; these are the predominant IL-1 cytokines that activate key transcription factors related to inflammatory immune responses [58,59]. It has been reported that IL-6 is a multifunctional cytokine, a prominent indicator of ongoing inflammation in the airways and an important regulator of effector CD4+ T cell fate [60]. In our study, we found that MA-challenged mice had significantly higher IL-6 and KC expression, which are clinically relevant, and suggests that both cause lung injury by increasing the infiltration of neutrophils. Kp-10 has been reported to reduce the mRNA levels for inflammatory cytokines (IL-1β, IL-6, TNF-α) in RAW 264.7 cells [61]. Also, macrophages isolated from $Gpr54^{-/-}$ mice produced more pro-inflammatory cytokines after LPS stimulation as compared with those in $Gpr54^{+/+}$ mice [62]. Similarly, in our study, we observed a suppression of notable pro-inflammatory cytokines in all the study populations, suggesting the significant role of Kp/KISS1R signaling in regulating the inflammatory milieu of the lungs. However, the signaling mechanisms through which Kp-10 exerted its anti-inflammatory effect is not clear. Studies have shown that NF-κB and MAPK signaling pathways are important to induce inflammatory cytokines expression [63]. The mechanistic basis of Kp effects on the immune system should be further explored in future studies. Furthermore, we observed a more pronounced effect of Kp-10 in alleviating the MA-induced inflammatory response in the presence of endogenous estrogen (in female mice), suggesting estrogen signaling is required in combination with exogenous Kp-10 to enhance the protective mechanism to regulate the inflammatory milieu.

Prolonged exposure to allergens increases the inflammatory responses in the airways that cause airway structural changes and are associated with increased collagen deposition, immune cell recruitments, and airway thickening [39,64–66]. We observed increased cytokines levels and histology changes like ASM and epithelial thickening, collagen deposition, and goblet cell hyperplasia in MA-challenged mice. In our histology studies, we observed that MA-challenged mice showed a significant deterioration in the airway structures, which aligns with the AHR and remodeling [15]. Collagen is one of the primary structural components of airway ECM and is important for regeneration and repair [67,68]. The increased infiltration of inflammatory cells coupled with structural alterations in the airway leads to an increase in collagen deposition results in an increase in matrix stiffness [67]. The observed increase in airway stiffness in the MA-challenged mice may decrease the stretching, thereby influencing bronchodilation that overall reflects in AHR [69,70]. In our data, we observed elevated soluble collagen levels in MA-challenged mice, suggesting increased ECM and lung tissue remodeling. However, this effect was ablated with Kp-10 treatment, suggesting that Kp-10's anti-remodeling effects are via inhibition of collagen deposition in the lungs, and this is corroborated with Kp's anti-fibrotic activity in bleomycin-induced pulmonary fibrosis mouse model [71]. In addition, other matrix proteins including collagens undergo post-translational modifications to induce collagen cross-linking and thereby increasing airway stiffness and rigidity [67]. Vimentin, a marker

for fibrosis, and α-SMA, a smooth muscle-specific marker were also found to be increased in asthmatic lungs, signifying the airway structural changes during remodeling in the airways. These changes were reversed upon Kp-10 treatment in MA-challenged mice, suggesting that Kp-10 has a promising potential in regulating remodeling-associated changes in the airways.

To summarize, the results of the present study show that MA significantly altered lung mechanics, resulting in AHR and airway remodeling. The administration of Kp-10 alleviated the MA-induced airway inflammation and remodeling, and thereby AHR. Furthermore, we observed a protective role of Kp/KISS1R signaling in asthmatic OVX mice, suggesting an estrogen-independent effect of Kp/KISS1R signaling. All of these findings indicate a critical protective role for Kp/KISS1R activation in regulating AHR and airway remodeling.

Supplementary Material

Refer to Web version on PubMed Central for supplementary material.

Acknowledgments

This work was supported by the National Heart, Lung, and Blood Institute (NHLBI), NIH/NHLBI R01-HL146705, and R01-HL146705-02S1 (to V.S.).

Data availability statement

The data supporting the conclusions of this article are included in this publication and/or its supplementary material.

References:

1. Postma DS, Timens W. Remodeling in asthma and chronic obstructive pulmonary disease. Proc Am Thorac Soc 2006; 3: 434–439. [PubMed: 16799088]
2. Prakash YS. Emerging concepts in smooth muscle contributions to airway structure and function: implications for health and disease. Am J Physiol Lung Cell Mol Physiol 2016; 311: L1113–L1140. [PubMed: 27742732]
3. Prakash YS. Airway smooth muscle in airway reactivity and remodeling: what have we learned? Am J Physiol Lung Cell Mol Physiol 2013; 305: L912–933. [PubMed: 24142517]
4. Ambhore NS, Katragadda R, Raju Kalidhindi RS, et al. Estrogen receptor beta signaling inhibits PDGF induced human airway smooth muscle proliferation. Mol Cell Endocrinol 2018; 476: 37–47. [PubMed: 29680290]
5. Borkar NA, Roos B, Prakash YS, et al. Nicotinic alpha7 acetylcholine receptor (alpha7nAChR) in human airway smooth muscle. Arch Biochem Biophys 2021; 706: 108897. [PubMed: 34004182]
6. Kalidhindi RSR, Borkar NA, Ambhore NS, et al. Sex steroids skew ACE2 expression in human airway: a contributing factor to sex differences in COVID-19? Am J Physiol Lung Cell Mol Physiol 2020; 319: L843–L847. [PubMed: 32996784]
7. Borkar NA, Combs CK, Sathish V. Sex Steroids Effects on Asthma: A Network Perspective of Immune and Airway Cells. Cells 2022; 11: 2238. [PubMed: 35883681]
8. Sathish V, Martin YN, Prakash YS. Sex steroid signaling: implications for lung diseases. Pharmacol Ther 2015; 150: 94–108. [PubMed: 25595323]
9. Townsend EA, Miller VM, Prakash YS. Sex differences and sex steroids in lung health and disease. Endocr Rev 2012; 33: 1–47. [PubMed: 22240244]

10. Banerjee P, Balraj P, Ambhore NS, et al. Network and co-expression analysis of airway smooth muscle cell transcriptome delineates potential gene signatures in asthma. Sci Rep 2021; 11: 1–16. [PubMed: 33414495]
11. Ambhore NS, Kalidhindi RSR, Sathish V. Sex-steroid signaling in lung diseases and inflammation. In: Lung Inflammation in Health and Disease, Volume I. Springer, 2021; 243–273.
12. Seymour BW, Friebertshauser KE, Peake JL, et al. Gender differences in the allergic response of mice neonatally exposed to environmental tobacco smoke. Dev Immunol 2002; 9: 47–54. [PubMed: 12353662]
13. Borkar NA, Sathish V. Sex steroids and their influence in Lung Diseases across the lifespan. In: Sex-Based Differences in Lung Physiology. 2021: 39–72.
14. Kotani M, Detheux M, Vandenbogaerde A, et al. The metastasis suppressor gene KiSS-1 encodes kisspeptins, the natural ligands of the orphan G protein-coupled receptor GPR54. J Biol Chem 2001; 276: 34631–34636. [PubMed: 11457843]
15. Ohtaki T, Shintani Y, Honda S, et al. Metastasis suppressor gene KiSS-1 encodes peptide ligand of a G-protein-coupled receptor. Nature 2001; 411: 613–617. [PubMed: 11385580]
16. Muir AI, Chamberlain L, Elshourbagy NA, et al. AXOR12, a novel human G protein-coupled receptor, activated by the peptide KiSS-1. J Biol Chem 2001; 276: 28969–28975. [PubMed: 11387329]
17. Lee DK, Nguyen T, O'Neill GP, et al. Discovery of a receptor related to the galanin receptors. FEBS letters 1999; 446: 103–107. [PubMed: 10100623]
18. Franssen D, Tena-Sempere M. The kisspeptin receptor: A key G-protein-coupled receptor in the control of the reproductive axis. Best Pract Res Clin Endocrinol Metab 2018; 32: 107–123. [PubMed: 29678280]
19. Sanchez-Garrido MA, Tena-Sempere M. Metabolic control of puberty: roles of leptin and kisspeptins. Horm Behav 2013; 64: 187–194. [PubMed: 23998663]
20. Roa J, Aguilar E, Dieguez C, et al. New frontiers in kisspeptin/GPR54 physiology as fundamental gatekeepers of reproductive function. Front Neuroendocrinol 2008; 29: 48–69. [PubMed: 17870152]
21. d'Anglemont de Tassigny X, Colledge WH. The role of kisspeptin signaling in reproduction. Physiology (Bethesda) 2010; 25: 207–217. [PubMed: 20699467]
22. Seminara SB, Messager S, Chatzidaki EE, et al. The GPR54 gene as a regulator of puberty. N Engl J Med 2003; 349: 1614–1627. [PubMed: 14573733]
23. Gaytan F, Gaytan M, Castellano JM, et al. KiSS-1 in the mammalian ovary: distribution of kisspeptin in human and marmoset and alterations in KiSS-1 mRNA levels in a rat model of ovulatory dysfunction. Am J Physiol Endocrinol Metab 2009; 296: E520–531. [PubMed: 19141682]
24. Borkar NA, Ambhore NS, Kalidhindi RSR, et al. Kisspeptins inhibit human airway smooth muscle proliferation. JCI Insight 2022; 7.
25. National Research Council, Guide for the care and use of laboratory animals. Eighth edition 2010; The National Academies Press, Washington, DC.
26. Kalidhindi RSR, Ambhore NS, Balraj P, et al. Androgen receptor activation alleviates airway hyperresponsiveness, inflammation, and remodeling in a murine model of asthma. Am J Physiol Lung Cell Mol Physiol 2021; 320: L803–L818. [PubMed: 33719566]
27. Kalidhindi RSR, Ambhore NS, Bhallamudi S, et al. Role of Estrogen Receptors alpha and beta in a Murine Model of Asthma: Exacerbated Airway Hyperresponsiveness and Remodeling in ERbeta Knockout Mice. Front Pharmacol 2019; 10: 1499. [PubMed: 32116656]
28. Ambhore NS, Kalidhindi RSR, Loganathan J, et al. Role of Differential Estrogen Receptor Activation in Airway Hyperreactivity and Remodeling in a Murine Model of Asthma. Am J Respir Cell Mol Biol 2019; 61: 469–480. [PubMed: 30958966]
29. Takeda T, Kikuchi E, Mikami S, et al. Prognostic role of KiSS-1 and possibility of therapeutic modality of metastin, the final peptide of the KiSS-1 gene, in urothelial carcinoma. Mol Cancer Ther 2012; 11: 853–863. [PubMed: 22367780]

30. Yarova PL, Stewart AL, Sathish V, et al. Calcium-sensing receptor antagonists abrogate airway hyperresponsiveness and inflammation in allergic asthma. Sci Transl Med 2015; 7: 284ra260–284ra260.
31. Kalidhindi RSR, Ambhore NS, Sathish V. Cellular and Biochemical Analysis of Bronchoalveolar Lavage Fluid from Murine Lungs. Methods Mol Biol 2021; 2223: 201–215. [PubMed: 33226597]
32. Cho JY, Miller M, Baek KJ, et al. Immunostimulatory DNA sequences inhibit respiratory syncytial viral load, airway inflammation, and mucus secretion. J Allergy Clin Immunol 2001; 108: 697–702. [PubMed: 11692091]
33. Setlakwe EL, Lemos KR, Lavoie-Lamoureux A, et al. Airway collagen and elastic fiber content correlates with lung function in equine heaves. Am J Physiol Lung Cell Mol Physiol 2014; 307: L252–L260. [PubMed: 24879055]
34. Ambhore NS, Kalidhindi RSR, Pabelick CM, et al. Differential estrogen-receptor activation regulates extracellular matrix deposition in human airway smooth muscle remodeling via NF-kappaB pathway. FASEB J 2019; 33: 13935–13950. [PubMed: 31638834]
35. Loganathan J, Pandey R, Ambhore NS, et al. Laser-capture microdissection of murine lung for differential cellular RNA analysis. Cell Tissue Res 2019; 376: 425–432. [PubMed: 30710174]
36. Schaafsma D, Dueck G, Ghavami S, et al. The mevalonate cascade as a target to suppress extracellular matrix synthesis by human airway smooth muscle. Am J Respir Cell Mol Biol 2011; 44: 394–403. [PubMed: 20463291]
37. Nayak AP, Deshpande DA, Shah SD, et al. OGR1-dependent regulation of the allergen-induced asthma phenotype. Am J Physiol Lung Cell Mol Physiol 2021; 321: L1044–l1054. [PubMed: 34668419]
38. Ambhore NS, Kumar A, Sathish V. Molecular determinants of airway smooth muscle cells in health and disease. Ann Transl Med 2022; 10: 1084. [PubMed: 36388811]
39. Kudo M, Ishigatsubo Y, Aoki I. Pathology of asthma. Front Microbiol 2013; 4: 263. [PubMed: 24032029]
40. Araujo BB, Dolhnikoff M, Silva LF, et al. Extracellular matrix components and regulators in the airway smooth muscle in asthma. Eur Respir J 2008; 32: 61–69. [PubMed: 18321931]
41. Wang R, Wang Y, Liao G, et al. Abi1 mediates airway smooth muscle cell proliferation and airway remodeling via Jak2/STAT3 signaling. iScience 2022; 25: 103833. [PubMed: 35198891]
42. Harter CJ, Kavanagh GS, Smith JT. The role of kisspeptin neurons in reproduction and metabolism. J Endocrinol 2018; 238: R173–R183. [PubMed: 30042117]
43. Cvetković D, Babwah AV, Bhattacharya M. Kisspeptin/KISS1R system in breast cancer. J Cancer 2013; 4: 653. [PubMed: 24155777]
44. Harihar S, Ray S, Narayanan S, et al. Role of the tumor microenvironment in regulating the anti-metastatic effect of KISS1. Clin Exp Metastasis 2020; 37: 209–223. [PubMed: 32088827]
45. Guzman S, Brackstone M, Radovick S, et al. KISS1/KISS1R in cancer: friend or foe? Front Endocrinol 2018; 9: 437.
46. Guzman S, Brackstone M, Wondisford F, et al. KISS1/KISS1R and breast cancer: metastasis promoter. Semin Reprod Med 2019; 37: 197–206. [PubMed: 31972865]
47. Blake A, Dragan M, Tirona RG, et al. G protein-coupled KISS1 receptor is overexpressed in triple negative breast cancer and promotes drug resistance. Sci Rep 2017; 7: 1–17. [PubMed: 28127051]
48. Xoxakos I, Petraki C, Msauel P, et al. Expression of Kisspeptin (KISS1) and its Receptor GPR54 (KISS1R) in Prostate Cancer. Anticancer Res 2020; 40: 709–718. [PubMed: 32014912]
49. d'Anglemont de Tassigny X, Jayasena CN, Murphy KG, et al. Mechanistic insights into the more potent effect of KP-54 compared to KP-10 in vivo. PLoS One 2017; 12: e0176821. [PubMed: 28464043]
50. Kotani M, Mollereau C, Detheux M, et al. Functional characterization of a human receptor for neuropeptide FF and related peptides. Br J Pharmacol 2001; 133: 138–144. [PubMed: 11325803]
51. Li D, Mitchell D, Luo J, et al. Estrogen regulates KiSS1 gene expression through estrogen receptor α and SP protein complexes. Endocrinology 2007; 148: 4821–4828. [PubMed: 17656465]
52. Smith JT, Cunningham MJ, Rissman EF, et al. Regulation of Kiss1 gene expression in the brain of the female mouse. Endocrinology 2005; 146: 3686–3692. [PubMed: 15919741]

53. Ghadiali S, Huang Y. Role of airway recruitment and derecruitment in lung injury. Crit Rev Biomed Eng 2011; 39: 297–317. [PubMed: 22011235]
54. Devos FC, Maaske A, Robichaud A, et al. Forced expiration measurements in mouse models of obstructive and restrictive lung diseases. Respir Res 2017; 18: 123. [PubMed: 28629359]
55. Paré PD. Central airway compliance in asthma: up or down? Good or bad? Am J Respir Crit Care Med 2011; 183: 563–564. [PubMed: 21471052]
56. Chen L, Deng H, Cui H, et al. Inflammatory responses and inflammation-associated diseases in organs. Oncotarget 2018; 9: 7204. [PubMed: 29467962]
57. Sharma P, Yi R, Nayak AP, et al. Bitter Taste Receptor Agonists Mitigate Features of Allergic Asthma in Mice. Sci Rep 2017; 7: 46166. [PubMed: 28397820]
58. Rex J, Lutz A, Faletti LE, et al. IL-1β and TNFα differentially influence NF-κB activity and FasL-induced apoptosis in primary murine hepatocytes during LPS-induced inflammation. Front Physiol 2019; 10: 117. [PubMed: 30842741]
59. Rex J, Albrecht U, Ehlting C, et al. Model-based characterization of inflammatory gene expression patterns of activated macrophages. PLoS Comput Biol 2016; 12: e1005018. [PubMed: 27464342]
60. Rincon M, Irvin CG. Role of IL-6 in asthma and other inflammatory pulmonary diseases. Int J Biol Sci 2012; 8: 1281. [PubMed: 23136556]
61. Wang G, Petzke MM, Iyer R, et al. Pattern of proinflammatory cytokine induction in RAW264.7 mouse macrophages is identical for virulent and attenuated Borrelia burgdorferi. J Immunol 2008; 180: 8306–8315. [PubMed: 18523297]
62. Wang D, Wu Z, Zhao C, et al. KP-10/Gpr54 attenuates rheumatic arthritis through inactivating NF-κB and MAPK signaling in macrophages. Pharmacol Res 2021; 171: 105496. [PubMed: 33609696]
63. Kawai T, Akira S. The role of pattern-recognition receptors in innate immunity: update on Toll-like receptors. Nat Immunol 2010; 11: 373–384. [PubMed: 20404851]
64. Murdoch JR, Lloyd CM. Chronic inflammation and asthma. Mutat Res 2010; 690: 24–39. [PubMed: 19769993]
65. Djukanovic R Airway inflammation in asthma and its consequences: implications for treatment in children and adults. J Allergy Clin Immunol 2002; 109: S539–S548. [PubMed: 12063510]
66. Fahy JV. Type 2 inflammation in asthma—present in most, absent in many. Nat Rev Immunol 2015; 15: 57–65. [PubMed: 25534623]
67. Liu L, Stephens B, Bergman M, et al. Role of collagen in airway mechanics. Bioengineering 2021; 8: 13. [PubMed: 33467161]
68. Palmans E, Pauwels RA, Kips JC. Repeated allergen exposure changes collagen composition in airways of sensitised Brown Norway rats. Eur Respir J 2002; 20: 280–285. [PubMed: 12212956]
69. Ansell T, McFawn P, Noble P, et al. Potent bronchodilation and reduced stiffness by relaxant stimuli under dynamic conditions. Eur Respir J 2009; 33: 844–851. [PubMed: 19010981]
70. Fredberg JJ, Inouye D, Miller B, et al. Airway smooth muscle, tidal stretches, and dynamically determined contractile states. Am J Respir Crit Care Med 1997; 156: 1752–1759. [PubMed: 9412551]
71. Lei Z, Bai X, Ma J, et al. Kisspeptin13 inhibits bleomycininduced pulmonary fibrosis through GPR54 in mice. Mol Med Rep 2019; 20: 1049–1056. [PubMed: 31173221]

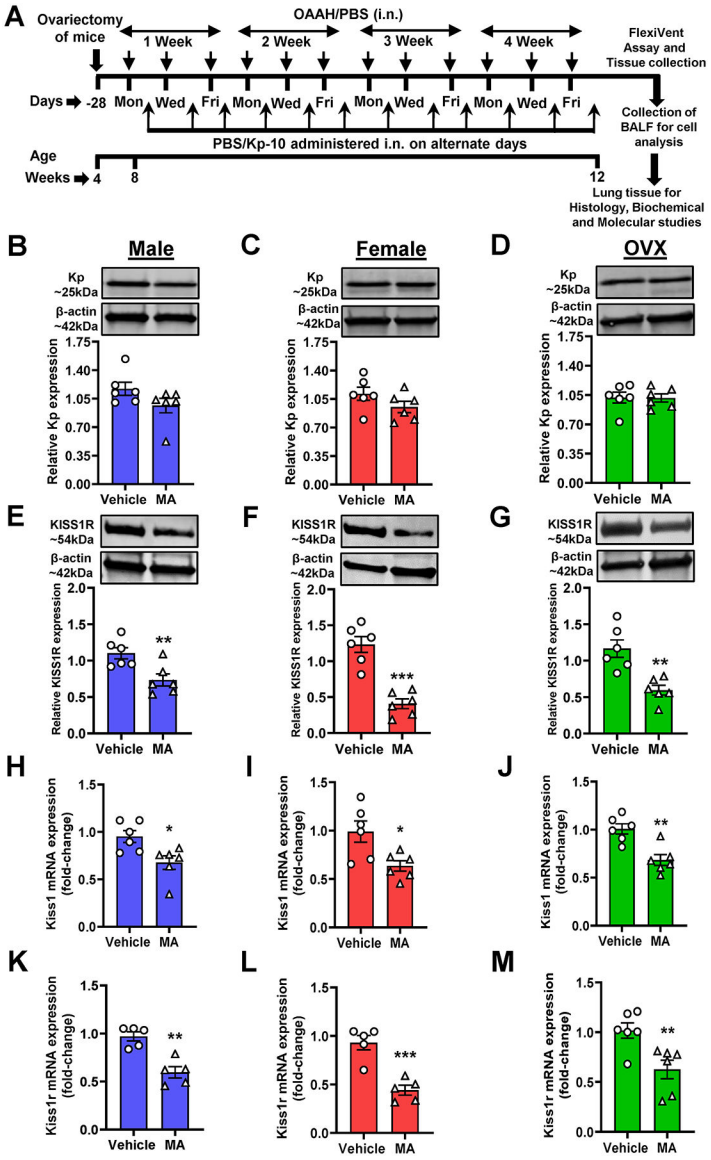

Figure 1.

Schematic showing the experimental design of the study. Mice were sensitized with mixed allergen (MA, OAAH: 10 μg each of Ovalbumin, *Alternaria alternata, Aspergillus fumigatus,* and *Dermatophagoides farinae* (house dust mite)) or Dulbecco's phosphate-buffered saline, DPBS, vehicle) intranasally (i.n.) on alternate days (starting from day 1) for 4 weeks (3 days/week). From day 2 onward, on alternate days (3 days/week), mice in the respective groups received DPBS or Kisspeptin-10 (Kp-10) by intranasal administration. Ovariectomy (OVX) surgery was performed at the age of 4-weeks (A). Kisspeptin (Kp) and KISS1R protein expression were measured in whole lung tissue of DPBS and MA-challenged mice (male (B and E), female (C and F), and OVX (D and G)). Further, airway smooth muscle (ASM) bundle was isolated from the lung using laser capture microdissection-assisted microscopy and RNA was isolated. Subsequently, specific ASM *Kiss1* and *Kiss1r* mRNA levels were measured using RT-PCR in male (H and K), female (I

and L), and OVX (J and M) mice. Data were analyzed using a two-tailed unpaired Student's *t*-test. Mean ± SEM (n=5 or 6 mice/group); *p<0.05, **p<0.01, ***p<0.001

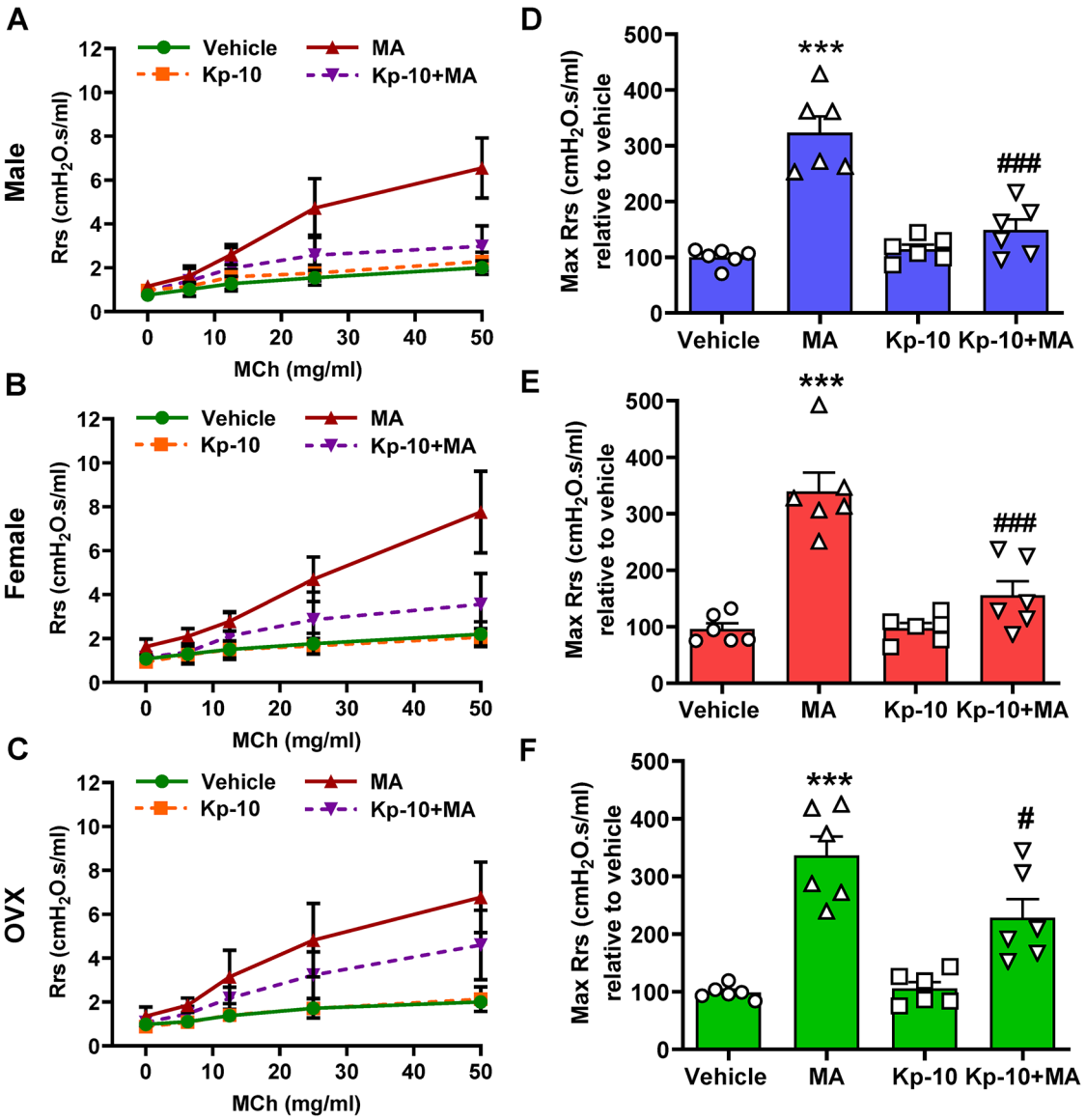

Figure 2.

Effects of Kp-10 on total respiratory system resistance (Rrs) in a MA model of asthma in male (A), female (B), and OVX (C) mice. The response to inhaled increasing concentrations of methacholine (MCh) (0–50 mg/ml) were measured in anesthetized animals using a flexiVent system (A–C). Max Rrs at the concentration of 50 mg/ml of MCh was used to compare the effectiveness of the treatment groups (male (D), female (E), and OVX (F) mice). MA challenged mice from all three study populations showed a robust increase in Max Rrs compared to the baseline value (DPBS-challenge). This effect of MA was alleviated in mice treated with Kp-10 in all three study populations. Data were analyzed using two-way ANOVA followed by Tukey's *post hoc* test. Mean ± SEM (n=6 mice/group); ***$p<0.001$ versus respective vehicle group; $^{\#}p<0.05$, $^{\#\#\#}p<0.001$ versus respective MA-challenged group.

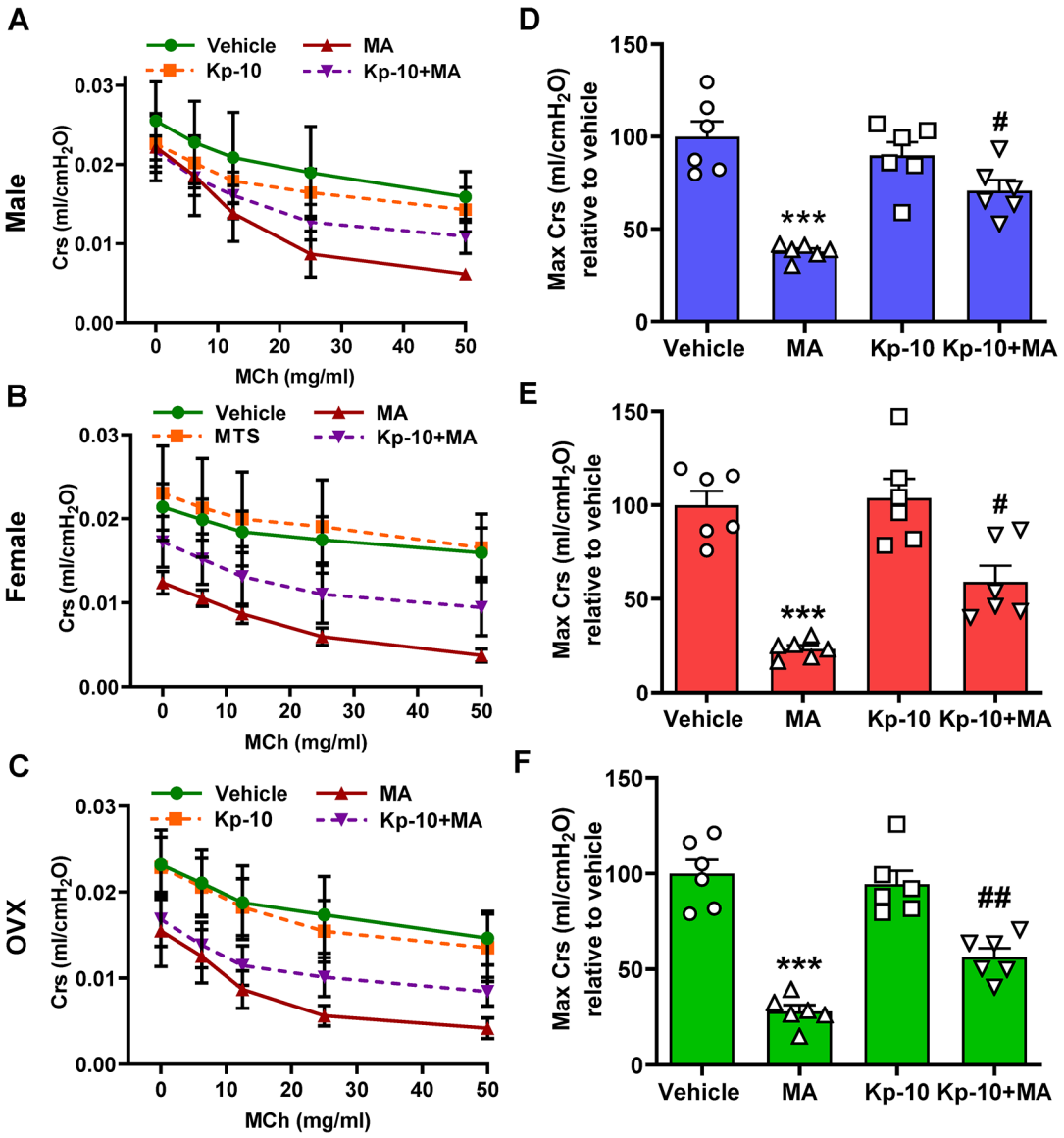

Figure 3.

Effect of Kp-10 on total respiratory system compliance (Crs) in a MA model of asthma in male (A), female (B), and OVX (C) mice. Crs at increasing MCh concentrations from 0–50 mg/ml were measured in anesthetized animals using a flexiVent system (A–C). Max Crs at the concentration of 50 mg/ml MCh was used to compare the effectiveness of the treatment groups (male (D), female (E), and OVX (F) mice). MA-challenged mice from all three study populations showed a significant decrease in Max Crs compared to the baseline value (DPBS-challenge). This effect of MA was alleviated in mice treated with Kp-10 in all three study populations. Data were analyzed using two-way ANOVA followed by Tukey's *post hoc* test. Mean ± SEM (n=6 mice/group); ***$p<0.001$ versus respective vehicle group; $^{\#}p<0.05$, $^{\#\#}p<0.01$ versus respective MA-challenged group.

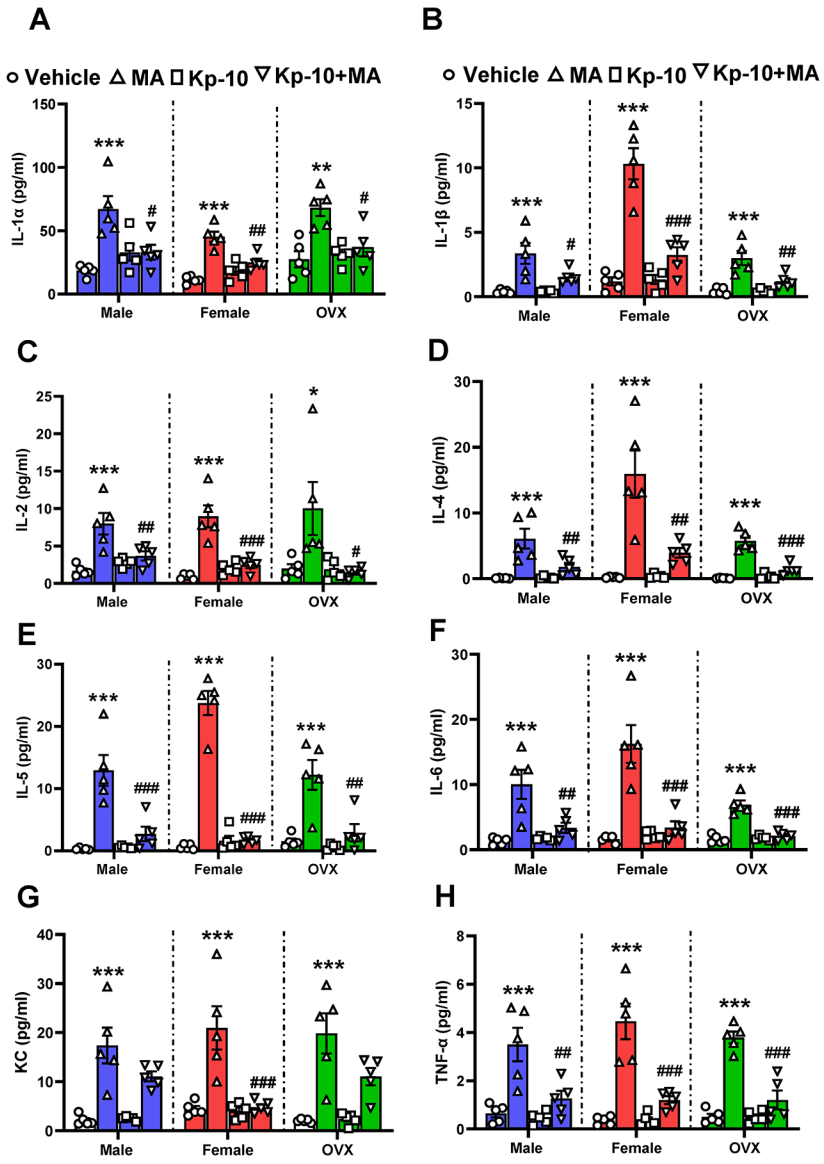

Figure 4.

Effect of Kp-10 on cytokine levels in bronchoalveolar lavage fluids (BALF). MA-challenge showed an increase in IL-1α (A), IL-1β (B), IL-2 (C), IL-4 (D), IL-5 (E), IL-6 (F), KC (G) and TNF-α (H) levels in a BALF collected from the lungs of male, female and OVX mice compared with the respective DPBS-challenged mice. MA-induced increases in Th2 cytokines in all three study populations (male, female and OVX) were decreased with Kp-10 treatment. Data analyzed using two-way ANOVA followed by Tukey's *post hoc* test. Mean ± SEM (n=5 mice/group); *p<0.05, **p<0.01, ***p<0.001 versus respective vehicle group; $^{\#}$p<0.05, $^{\#\#}$p<0.01, $^{\#\#\#}$p<0.001 versus respective MA-challenged group.

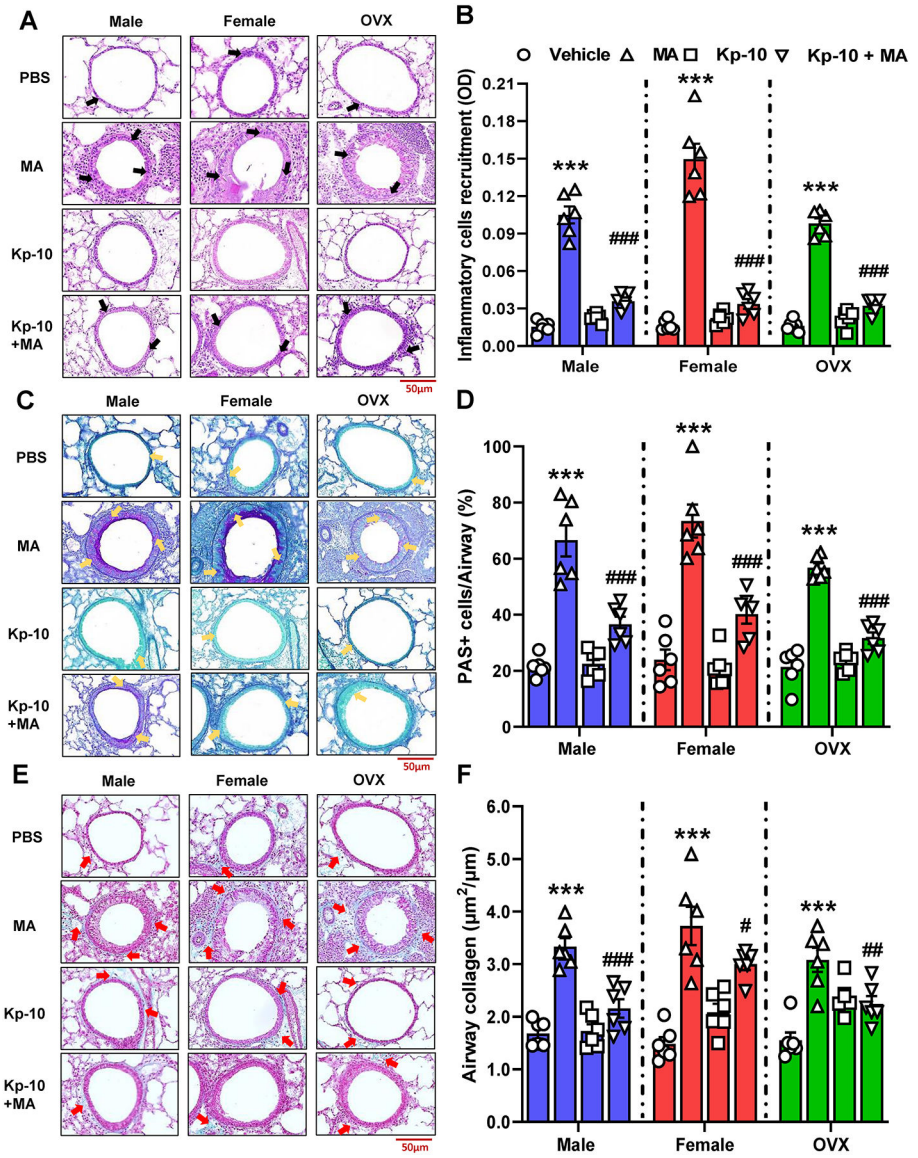

Figure 5.

Effects of Kp-10 on lung histology. Representative images of lung sections from MA-challenged male, female, and OVX mice show increased inflammatory cell infiltration in the airways (H&E staining; A), higher total number of PAS-positive epithelial cells per airways (yellow arrow; C) and increased collagen deposition around the airways (red arrows; E). This effect of MA on deteriorating the lung histology was alleviated in mice treated with Kp-10 in all three study populations (A–F). Data analyzed using two-way ANOVA followed by Tukey's *post hoc* test. Mean ± SEM (n=6/group); ***p<0.001 versus respective vehicle group; $^{\#}$p<0.05, $^{\#\#}$p<0.01, $^{\#\#\#}$p<0.001 versus respective MA-challenged group; scale bar: 50 μm.

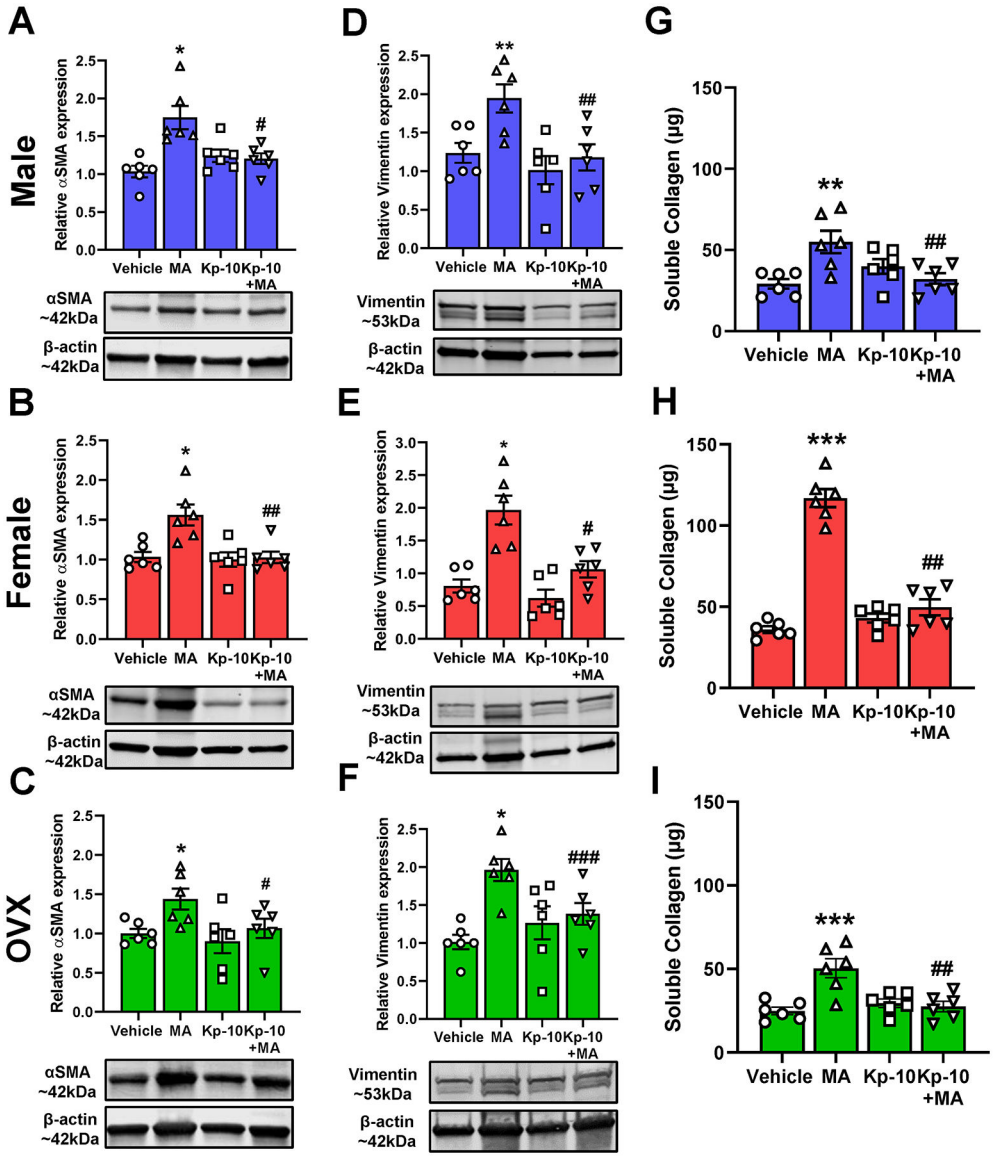

Figure 6.

Effects of Kp-10 on α-smooth muscle actin (α-SMA), vimentin and soluble collagen levels in the lung. The protein expression of α-SMA and vimentin were increased upon MA-challenge, and this effect was reversed by Kp-10 treatment in male (A and D), female (B and E), and OVX (C and F) mice lung homogenate. Soluble collagen levels were increased in the lung tissue lysates from MA-challenged male (G), female (H) and OVX (I) mice. Data analyzed using one-way repeated measures ANOVA followed by Tukey's *post hoc* test. Mean ± SEM (n=6 mice/group); *p<0.05, **p<0.01, ***p<0.001 versus respective vehicle; #p<0.05, ##p<0.01, ###p<0.001 versus respective MA-challenged group.